



# Recent trace element contamination in a rural crater lake, NW Mexico

A. C. Ruiz-Fernández · J. A. Sanchez-Cabeza · L. H. Pérez-Bernal · M. Blaauw · J. G. Cardoso-Mohedano · M. A. Aquino-López · S. Giralt

Received: 11 December 2020 / Accepted: 25 August 2022 / Published online: 17 October 2022  
© The Author(s), under exclusive licence to Springer Nature B.V. 2022

**Abstract** Lakes provide a wide range of ecosystem services that are increasingly at risk because of multiple anthropogenic pressures. Santa María del Oro crater lake lies in rural northwest Mexico and is of interest for global change studies and as a natural resource that sustains the economies of local communities. Temporal trends of trace element (As, Co, Cr, Cu, Ni, Pb, V, and Zn) concentrations over the past century were assessed in four  $^{210}\text{Pb}$ -dated sediment cores, under the hypothesis that recent anthropogenic activities have promoted increasing trace element inputs. Data were analyzed within three

periods: (1) pre-1900s, from which background levels were estimated, (2) pre-1950, and (3) post-1950. Trace element provenance was determined through a chemometric approach. Most trace element concentrations varied little in the past ~100 years, with no Co, V, and Zn enrichment, and minor enrichment by Cr, Cu, Ni and Pb in a few sections of the cores collected from the deepest locations, within the hypolimnion, and by Pb along the shallowest core. In contrast, As enrichment in the deep cores reached moderately severe levels during the post-1950 period. Cobalt, Pb, V, and Zn input to the lake was related to terrigenous sources. Lead enrichment was mainly anthropogenic (the shallow coring site is close to human settlements). Copper and Cr variability were mostly

**Supplementary Information** The online version contains supplementary material available at <https://doi.org/10.1007/s10933-022-00268-3>.

A. C. Ruiz-Fernández (✉) · J. A. Sanchez-Cabeza · L. H. Pérez-Bernal  
Instituto de Ciencias del Mar y Limnología, Unidad Académica Mazatlán, Universidad Nacional Autónoma de México, Calz. Joel Montes Camarena s/n, Col. Playa Sur, 82040 Mazatlán, Sin., Mexico  
e-mail: caro@ola.icmyl.unam.mx

J. A. Sanchez-Cabeza  
e-mail: jasanchez@cmarl.unam.mx

L. H. Pérez-Bernal  
e-mail: lbernal@ola.icmyl.unam.mx

M. Blaauw  
School of Natural and Built Environment,  
Queen's University Belfast, 42 Fitzwilliam Street,  
Belfast BT9 6AX, UK  
e-mail: maarten.blaauw@qub.ac.uk

J. G. Cardoso-Mohedano  
Instituto de Ciencias del Mar y Limnología,  
Universidad Nacional Autónoma de México, Estación El Carmen, Carretera Carmen-Puerto Real Km. 9.5, 24157 Ciudad del Carmen, Camp., Mexico  
e-mail: gcardoso@cmarl.unam.mx

M. A. Aquino-López  
Centro de Investigación en Matemáticas, Callejón Jalisco s/n, 36000 Guanajuato, Gto., Mexico  
e-mail: aquino@cimat.mx

S. Giralt  
Geosciences Barcelona (Geo3BCN-CSIC), Lluís Solé i Sabarís s/n, 08028 Barcelona, Spain  
e-mail: sgiralt@geo3bcn.csic.es

the result of diagenetic reactions. Arsenic enrichment, however, was attributed to biogeochemical cycling processes, likely exacerbated by drought conditions and enhanced calcite precipitation. Contradicting our hypothesis, recent anthropogenic impact on the lake's environmental quality was small. However, a preliminary assessment, based on international guidelines, indicated that As, Cr, and Ni concentrations could be harmful to benthic biota, even at background levels. High As concentrations could affect the aquatic food web and human health, the latter through fish consumption. Given predictions for increasing droughts in the area, which induce greater evaporation and lower water levels, this issue could worsen in the future. Further studies on As contamination in the lake are needed to better understand potential hazards and enhance response capacity. Such data must be part of conservation efforts and should be integrated into management policies to ensure the lake's sustainability.

**Keywords** Tropical crater lake · Trace elements · Lacustrine sediments · Arsenic contamination

## Introduction

Lakes provide a wide range of ecosystem services, such as water supply, biodiversity, fisheries resources, and scenic and cultural values. However, these water bodies are sensitive ecosystems that are subject to change under the influence of external factors in their watersheds, aquifers, and the atmosphere. These factors may be affected by human activities that cause lakes to undergo rapid changes, thereby influencing aquatic ecosystem functions (USGS 2020).

Input of allochthonous sediments impacts the water quality of receiving water bodies, not only by increasing water column turbidity, but also by serving as diffuse sources and sinks of many contaminants, including heavy metals (Ongley 1996). Depending on the biogeochemical processes that occur in aquatic ecosystems (e.g. formation of organic complexes, changes in pH, redox, and salinity), incoming sediments can release already accumulated heavy metals into the overlying water, thereby causing secondary pollution, which can affect their ecological status (Algül and Beyhan 2020). Lake sediments can also serve as effective archives of contamination and can

be used to infer historical trends of trace element accumulation (Ruiz-Fernández et al. 2004; Yang and Rose 2005; Smol 2008; Ontiveros-Cuadras et al. 2014; Lin et al. 2018; Pelletier et al. 2020).

Santa María del Oro Lake (SAMO) is a small crater lake in northwest Mexico, characterized by scenic beauty and surrounded by rural settlements where agriculture and cattle raising are the main economic activities. It is close to a small urban area that has experienced gradual development as a tourist destination for at least 40 years, which has accelerated since 1995. In a very short period, the area has been modified by poorly planned shoreline constructions (PO 2003). Tourism can play an important role in diversifying the rural economy, contributing to sustainability of the population (Nooripoor et al. 2021). Tourist activities, however, may indirectly affect the water body through catchment changes, or directly impact the shoreline and the lake water (Dokulil 2013), contributing to environmental changes, including contamination by trace elements. Furthermore, the negative effects of these impacts might be exacerbated by ongoing global warming that is already affecting in-lake dynamics of most of Earth's water bodies (Sahoo and Schladow 2008; Jeppesen et al. 2014).

Four  $^{210}\text{Pb}$ -dated sediment cores collected in SAMO (Ruiz-Fernández et al. 2022) were used to determine the background levels and reconstruct the temporal variations in trace element (As, Co, Cr, Cu, Ni, Pb, V, and Zn) concentrations and enrichment over the past century. We hypothesized that recent development of agriculture, cattle ranching, and tourism induced deterioration of the environmental quality in the lake, owing to increased trace element inputs, which would be reflected as sediment contamination. Information on background levels and temporal trends of trace elements is relevant to assess the contamination status of aquatic ecosystems, and this information can be used to develop conservation initiatives and lake-management practices designed to prevent or control detrimental changes, and thus ensure sustainable ecosystem services.

## Study site

SAMO is a maar lake that lies within an extinct volcanic crater, at 750 m above sea level (a.s.l.), in the Trans-Mexican Volcanic Belt (Fig. 1). It is in the Municipality of Santa María del Oro (23,477

inhabitants; INEGI 2017) in the Mexican State of Nayarit, where the main productive activities are agriculture, cattle ranching, and tourism. Some small areas are exploited for gold (Au) and silver (Ag) production (200 ton day<sup>-1</sup>; SGM 2020).

The lake is 2 km in diameter, has a surface area of 3.7 km<sup>2</sup>, and a maximum depth of 65 m (Serrano et al. 2002). It is a warm (22.9–31.1 °C water temperature) oligomictic lake that remains stratified most of the year, with a thermocline between 20 and 37 m depth, and has a short and incomplete mixing phase during winter (Cardoso et al. 2019). It shows dissolved oxygen stratification during almost the whole year, with anoxic deep waters (> 30 m). It contains slightly alkaline, moderately hard, mesotrophic waters (Caballero et al. 2013) where cyanobacterial blooms occur after turnover (Bustillos et al. 2020). The study area lies in a semi-warm sub-humid (A(C) zone; García 1973) with a well-defined rainy season from June to October. Meteorological records (1981–2010) from a nearby station (CONAGUA station 00018005 Cerro Blanco; ~960 m a.s.l., ~5 km west of SAMO; SMN 2020) indicate mean annual minimum and maximum temperatures of 12.3 and 29.6 °C, respectively, a mean annual rainfall of ~1146 mm, and a mean annual evaporation of ~1660 mm. The region was reportedly affected by strong to very strong droughts between 1950 and 1980 (Hernández Cerda and Valdez Madero 2004).

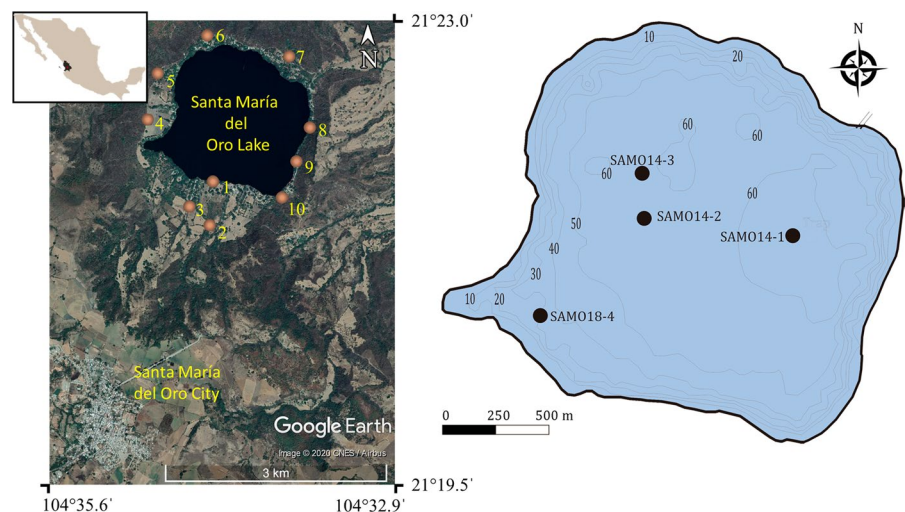
One important problem in SAMO’s surroundings is accelerated catchment erosion, associated with

agriculture, deforestation, and forest fires (PO 2003). Fires are induced by intense droughts, extreme temperatures, and uncontrolled domestic and agriculture waste burning (INIFAP 2012; SEDATU 2013). Besides supporting a growing tourism industry, the lake is used for sport and commercial fishing, and water is extracted for household, agricultural, and cattle ranching activities (PO 2003). The lake shoreline has undergone important modifications, owing to the construction of residential areas and tourism infrastructure, which have promoted a greater number of visitors (Moreno Moreno et al. 2015). SAMO has also been affected by the proliferation of tourist boats that use fossil fuels and by direct wastewater discharge, owing to the lack of sanitary drainage systems and wastewater treatment plants (PO 2003). It has also been used for cage-fish-farming projects (Valencia-Plascencia and Jácome-Pérez 1993) and receives surface runoff from the surrounding agricultural areas, including from the cultivation of blue agave for tequila production, since 1999 (González-Bernal 2008).

### Materials and methods

The methods used for sampling, <sup>210</sup>Pb dating, and sediment characterization of the four analyzed cores have been reported in detail (Ruiz-Fernández et al. 2022). Briefly, the cores were retrieved using a UWITEC™ gravity corer (86 mm inner diameter and 1.0-m-long transparent PVC tube). SAMO 14–1, SAMO 14–2,

**Fig. 1** Santa María del Oro Lake (SAMO), NW Mexico. Left: the inset shows Nayarit (black). Orange dots are the locations of soil samples. Right: deep cores SAMO 14–1 (21.369° N, 104.565° W, 55 m depth), SAMO 14–2 (21.370° N, 104.572° W, 48.2 m) and SAMO 14–3 (21.372° N, 104.572° W, 52 m), and shallow core SAMO 18–4 (21.371° N, 104.577° W, 30 m)



and SAMO 14–3 were collected in April 2014 at sampling depths of ~50 m, i.e. below the thermocline and hereafter referred to as deep cores. SAMO 18–4 was collected in May 2018 in 30 m water depth, i.e. near the thermocline, and is referred to as the shallow core (Fig. 1). The sediment cores were extruded and sectioned into 1-cm intervals (SAMO 14–1=84, SAMO 14–2=78, SAMO 14–3=91, and SAMO 18–4=36 sections). In May 2019, 10 surface soil samples were collected around SAMO (Fig. 1) by inserting PVC rings (10-cm diameter, 2-cm thick) into the soil. Soil samples were transferred to plastic bags with a plastic spatula. Sediment and soil samples were lyophilized and ground to powder with a porcelain mortar and pestle, except the aliquots used for grain size analysis.

For core dating, alpha particle spectrometry (Alpha Ensemble Ortec-Ametek) was used to determine total  $^{210}\text{Pb}$  ( $^{210}\text{Pb}_{\text{tot}}$ ; Ruiz-Fernández and Hillaire-Marcel 2009) and  $^{239+240}\text{Pu}$  activities, and gamma-ray spectrometry (OrtecHPGe well-detector) was used to determine  $^{226}\text{Ra}$  ( $^{210}\text{Pb}_{\text{sup}}$ ) and  $^{137}\text{Cs}$  activities (Ruiz-Fernández et al. 2014; Díaz Asencio et al. 2020). Excess  $^{210}\text{Pb}$  ( $^{210}\text{Pb}_{\text{ex}}$ ) was calculated as the difference between  $^{210}\text{Pb}_{\text{tot}}$  and  $^{210}\text{Pb}_{\text{sup}}$  activities.

All sediment and soil samples were analyzed for element composition, including trace elements. Samples were placed into low-density polyethylene cells with the bottom covered with Prolene® film, manually compressed with a Teflon® rod, and analyzed by X-ray fluorescence spectrometry (XRF, SPECTROLAB Xepos-3) under He atmosphere. All sediment samples were analyzed for grain size distribution by laser diffraction (Malvern Mastersizer 2000E). Total, organic and inorganic carbon concentrations ( $C_{\text{tot}}$ ,  $C_{\text{org}}$ , and  $C_{\text{inorg}}$ , respectively) were determined in at least 1 of every 3 cm along the cores, with an elemental analyzer (Vario Microcube Elementar™); sediment aliquots were treated with 1 M HCl and freeze-dried before  $C_{\text{org}}$  analysis; the  $C_{\text{inorg}}$  fraction was estimated as the difference between  $C_{\text{tot}}$  and  $C_{\text{org}}$ . Magnetic susceptibility was determined using a Bartington MS2 system coupled to a MSG<sub>2</sub> frequency sensor.

Analysis of certified reference materials provided results within the reported range of the recommended values: IAEA-300 for  $^{210}\text{Pb}$  and  $^{137}\text{Cs}$ , LKSD-1 (CanmetMINING) for element concentrations, QAS3002 (Quality audit standard, Malvern™) for grain size percentages, and soil 502–308 (Leco) for carbon

concentrations. Replicate analysis of a single sample ( $n=6$ ) yielded a coefficient of variation < 6% for element concentrations, < 5% for grain size fractions and  $C_{\text{org}}$  percentages, and < 10% for  $^{210}\text{Pb}$  and  $^{137}\text{Cs}$ .

## Data treatment

### Sediment dating

The  $^{210}\text{Pb}$ -derived chronologies and mass accumulation rates (MAR) were calculated with the constant flux (CF) model (Robbins 1978; Sanchez-Cabeza and Ruiz-Fernández 2012), and dating uncertainties were estimated by Monte Carlo simulation (Sanchez-Cabeza et al. 2014). As SAMO 18–4 was too short to reach the equilibrium depth (Electronic Supplementary Material [ESM] Fig. S1) and the dating with the CF model requires the total inventory of  $^{210}\text{Pb}_{\text{xs}}$ , the missing  $^{210}\text{Pb}_{\text{xs}}$  inventory was estimated using an independently dated reference layer (where the  $^{137}\text{Cs}$  maximum was observed, assumed to correspond to 1963). Activity profiles (ESM Fig. S1) of  $^{137}\text{Cs}$  in the deep cores and  $^{239+240}\text{Pu}$  (only in cores SAMO 14–2 and SAMO 18–4) were used for  $^{210}\text{Pb}$  age-model validation.

### Data analysis

For analysis, data were grouped as: (1) pre-1900, including core sections beyond the dating limit owing to the lack of  $^{210}\text{Pb}_{\text{ex}}$ , (2) pre-1950, for sediments accumulated from 1900 to 1950, and (3) post-1950, for sediments accumulated since 1950 (Ruiz-Fernández et al. 2022), representing lower and higher global economic development, respectively. The year 1950 was taken as a reference point, owing to the onset of the Great Acceleration (Steffen et al. 2005) and, potentially, the Anthropocene epoch (AWG 2019).

### Background element concentrations

Two approaches were used to estimate the background concentrations of trace elements in the sediment cores. First, we used the mean value of the element concentrations in sediments accumulated before 1900 (pre-1900 group) and second, we computed the background values from a distribution function to estimate, with statistical reliability, element concentrations driven by natural processes (Matschullat et al.

2000). This method included three steps: (1) identify the lower concentrations in the dataset, assumed to represent the natural background values (defined as the “reduced dataset”) between the minimum and the median value, which is not affected by outliers or skewed data; (2) create a modified version of the “reduced data set” with the original values (element concentrations  $\leq$  median) and new values (element concentrations  $>$  median), calculated as twice the median minus each of the original values in the data set; and (3) use the new data set to produce a distribution function from which the mean  $\pm$  standard deviation represents the normal range of the background concentration for each element.

### Enrichment factor

The degree of trace element contamination was evaluated through the normalized enrichment factor (EF; Buat-Menard and Chesselet 1979). This index is used to evaluate enrichment by trace elements above background levels in sediments and is considered to be the most widely used and successful enrichment indicator presently in use (Birch 2017). The EF was computed as the ratio of the trace element concentration in each core section to the background concentration of each element, with all concentrations normalized by their corresponding Al concentration. Aluminum is used as a chemical tracer of aluminosilicates in the detrital fraction of the sediments (Loring and Rantala 1992) and serves as a proxy for detrital input. Normalization with Al is used to correct for dilution and to assess the enrichment of the trace elements by non-detrital components (Van der Weijden 2002).

To assess the contamination status of the sediments, the EF values were classified according to Birch and Davies (2003):  $EF < 1$ –2 indicates no enrichment;  $2 < EF \leq 3$  minor enrichment;  $3 < EF \leq 5$  moderate enrichment;  $5 < EF \leq 10$  moderately severe enrichment;  $10 < EF \leq 25$  severe enrichment,  $25 < EF \leq 50$  very severe enrichment, and  $EF \geq 50$ , extremely severe enrichment.

### Lake sediment quality assessment

Lake sediment quality, defined as the ability of sediment to maintain a healthy benthic population (Birch 2017), was evaluated through comparison of As, Cr, Cu, Ni, Pb, and Zn with their probable effect level

(PEL) screening values in freshwater sediments (Buchman 2008). PEL values refer to concentrations above which adverse effects are expected to occur frequently (MacDonald et al. 1996). This comparison was undertaken to determine which trace elements in the lake sediment might have adverse impacts on biota and to establish if further site-specific investigation might be needed, e.g. biological and chemical testing.

### Statistical analysis

The statistical analyses included 22 variables: percentages of clay, silt, sand,  $C_{org}$ , and  $C_{inorg}$ , and the concentrations of Al, As, Ca, Co, Cr, Cu, Fe, Mn, Ni, Pb, Rb, S, Sr, Ti, V, Zn, and Zr. Factor analysis (FA) was used to identify variable associations, explore similarities among cores, and to infer the provenance of the trace elements, with 289 analyzed core sections in total. We followed a compositional data analysis (CoDa) approach, based on the use of centered logratio (CLR) coefficients (Filzmoser et al. 2018). Imputation of missing values and values below the detection limit, as well as the transformation of the original data to CLR coefficients, were performed with the R-package robCompositions (Templ et al. 2021). The suitability of the database for FA was evaluated through the Bartlett’s test of sphericity, and the Kaiser–Meyer–Olkin (KMO) test was used to determine the measure of sampling adequacy (MSA) (Hair et al. 2014). Significant variables for each factor were those with loadings  $\geq 0.55$ . FA was performed through Minitab® 15.

Analysis of variance (ANOVA) followed by Tukey *post-hoc* tests was used to test differences between mean variable values among cores and among periods within the cores. These analyses were performed on the CLR-transformed database, at the 95% confidence level ( $p < 0.05$ ).

## Results

### $^{210}\text{Pb}$ dating

The  $^{210}\text{Pb}$  dating results are presented in detail in Ruiz-Fernández et al. (2022). All cores provided non-monotonic  $^{210}\text{Pb}_{xs}$  activity depth profiles (ESM Fig. 1a);  $^{210}\text{Pb}_{xs}$  activities that departed from an

exponential decay trend were interpreted to be a consequence of sediment input variations (Krishnaswami et al. 1971), for which the age models and accumulation rates were obtained through the CF dating model, that enables inference of temporal variations in SAR and MAR (Sanchez-Cabeza and Ruiz-Fernández 2012). The age models spanned  $103 \pm 16$  yr at 25 cm in SAMO 14–1,  $97 \pm 8$  yr at 23 cm in SAMO 14–2,  $106 \pm 6$  yr at 37 cm in SAMO 14–3, and  $66 \pm 9$  yr at 36 cm (bottommost section) in SAMO 18–4.

According to the  $^{210}\text{Pb}$  age models, the  $^{137}\text{Cs}$  maximum in each core was found at similar  $^{210}\text{Pb}$ -dated time spans in the deep cores (SAMO 14–1: 16–17 cm, 1960–1965; SAMO 14–2: 16–17 cm, 1960–1965; SAMO 14–3: 28–29 cm, 1962–1964), consistent with the period of maximum  $^{137}\text{Cs}$  fallout (1962–1964) produced by nuclear weapon testing (Bianchi 2007), and thus corroborating the  $^{210}\text{Pb}$ -derived chronologies. In SAMO 18–4, the  $^{137}\text{Cs}$  maximum (29–30 cm) was used to estimate the missing  $^{210}\text{Pb}_{\text{xs}}$  inventory, and the age model was corroborated by using the maximum of  $^{239+240}\text{Pu}$  found at the same depth.

Mean MAR values in the pre-1950 period were comparable among the deep cores, ranging from  $0.02 \pm 0.01$  g cm<sup>-2</sup> yr<sup>-1</sup> in SAMO 14–2 to  $0.03 \pm 0.01$  g cm<sup>-2</sup> yr<sup>-1</sup> in SAMO 14–1. Data are not available for SAMO 18–4. In the post-1950 period, MAR values in the deep cores were comparable, from  $0.06 \pm 0.05$  g cm<sup>-2</sup> yr<sup>-1</sup> in SAMO 14–2 to  $0.13 \pm 0.08$  g cm<sup>-2</sup> yr<sup>-1</sup> in SAMO 14–3, but significantly lower than in core SAMO 18–4 ( $0.28 \pm 0.21$  g cm<sup>-2</sup> yr<sup>-1</sup>). In this period, all cores showed considerable MAR fluctuations, particularly after the 1980s, and asynchronous maxima (ESM Fig. 1b), although MAR values decreased toward the surface, with values in the topmost core sections mostly within the interval of the pre-1950 mean value, except for SAMO 14–3.

#### Sediment characteristics and element concentrations

The sediment cores were composed mainly of silt (60–91%), with variable percentages of clay (7–29%) and sand (0–32%). According to ANOVA, the concentrations of Ca, C<sub>inorg</sub>, Sr, and Zr were comparable among cores (Fig. 2; Table 1), whereas the highest mean values of Pb, V, and Zn, and the lowest of silt, C<sub>org</sub>, Mn, S, and As were found in the shallow core

(SAMO 18–4), collected closest to lake shoreline (Fig. 1).

Temporal profiles of most variables (Fig. 3) were similar among the cores. The grain size fractions showed small variations (<10% for each grain size fraction), although the deep cores showed more scattered profiles than SAMO 18–4. During the pre-1950 period, the depth profiles generally showed decreasing concentrations of Al, Ti, Rb, Zr, Fe, Mn, and most trace elements (As, Co, Cr, Cu, Ni, Pb, V, and Zn), as well as increasing Ca and Sr concentrations; but during the post-1950 period, the records are noisier, with recurrent subsurface minima and maxima. Significant differences ( $p < 0.05$ ) in mean concentrations by period of some elements were consistently observed only in the deep cores (Fig. 4), with values of As being higher, and values of Co, Cr, Pb, V, and Zn being lower, during the post-1950 period than the pre-1900 period. Data are not available for pre-1900 period in SAMO 18–4. Grain size distribution, C<sub>org</sub> content, and most element concentrations in the pre-1900 segment were comparable among the cores, except for As and Ni concentrations, which were significantly higher ( $p < 0.05$ ) in SAMO 14–2 than in the other two cores (ESM Fig. S2).

Background element concentrations were estimated from cores SAMO 14–1, SAMO 14–2, and SAMO 14–3, since core SAMO 18–4 lacked a pre-1900 segment; the background values obtained from both methodologies (BC and BC<sub>M</sub>; Table 1, ESM Fig. S3) were comparable for each element ( $p > 0.05$ ).

#### Sediment quality assessment and enrichment factors

Benchmark PEL values were exceeded only by As in all cores (including the background values), and in some pre-1900 sections by Ni in SAMO 14–2 and SAMO 14–3, and by Cr in SAMO 14–3 (Table 1).

The enrichment factors, calculated using the BC values in each core, were <2 for most elements (Fig. 5). A few exceptions, observed mostly within the post-1950 period, include: SAMO 14–1 (2.2–5.0 for As, 2.1–2.2 for Cu and 2.3 for Pb in a single section); SAMO 14–2 (2.1–7.5 for As, 2.0–3.9 for Cu and 2.0–3.8 for Ni); SAMO 14–3 (2.0–5.8 for As, 2.0–2.3 for Cr and 2.0–2.1 for Cu, and 2.2 for Pb in a single section) and SAMO 18–4 (2.7 in a single section for Cu and 2.0–3.0 for Pb).

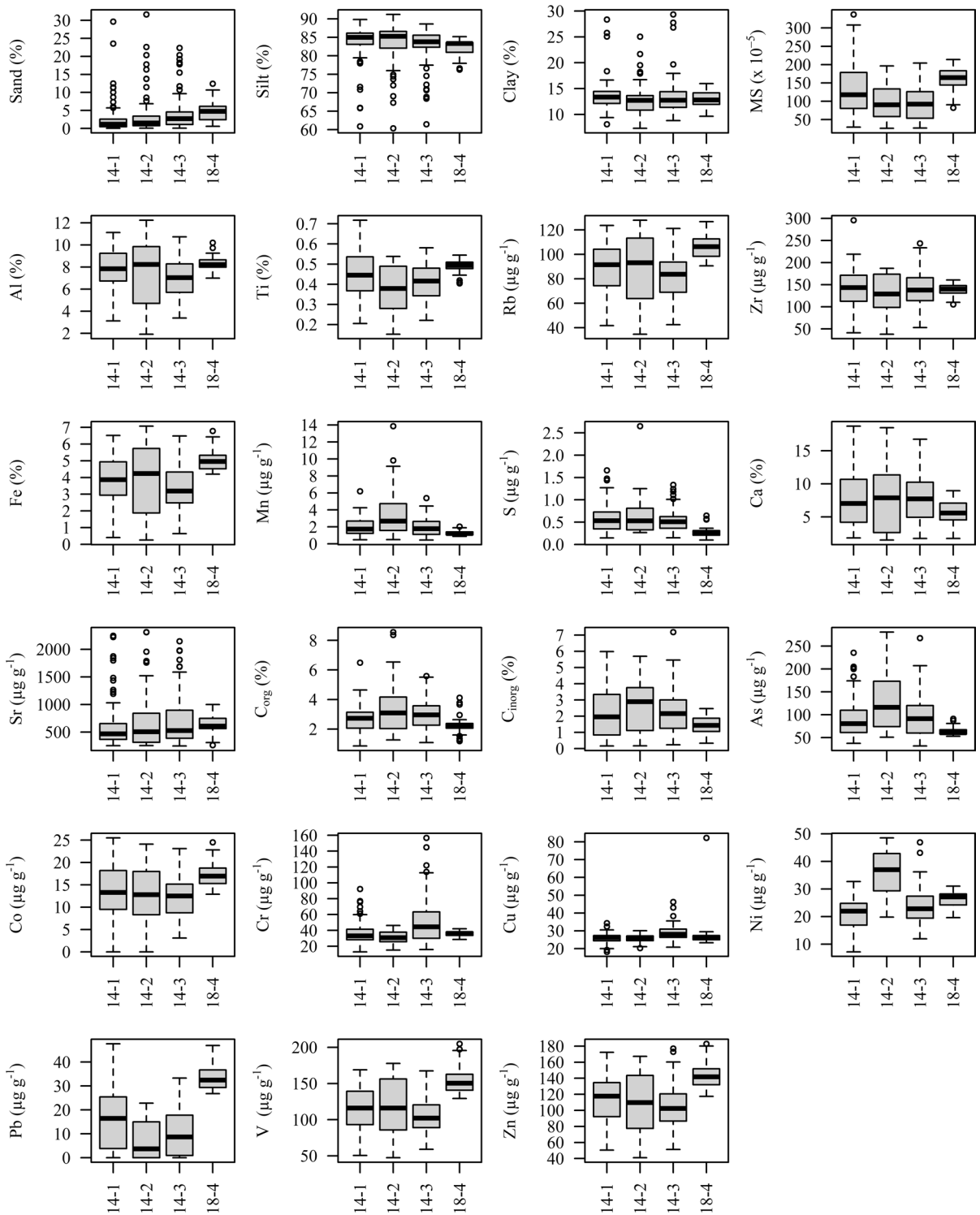


**Fig. 2** Boxplots of grain size distribution, magnetic susceptibility (MS), organic and inorganic carbon, and element concentrations in sediment cores from Santa María del Oro Lake, Mexico

**Table 1** Summary of sediment characteristics, element composition, and background values in sediment cores from Santa María del Oro Lake, NW Mexico

	Sand	Silt	Clay	MS	Al	Ti	Rb	Zr	Fe	Mn	S	
<i>Core</i>	<i>SAMO 14-1</i>											
N	83	84	84	84	84	84	84	84	84	84	84	
Min	<DL	60.9	8.1	29.5	3.1	0.2	41.7	41.2	0.4	0.5	0.1	
Max	29.6	89.8	28.4	337	11.1	0.7	124	296	6.5	6.2	1.7	
Mean	2.8	83.6	13.6	136	7.9	0.4	88.5	141	3.8	2.0	0.6	
SD	4.7	4.9	3.0	72.7	1.8	0.1	20.2	44.4	1.4	1.0	0.3	
<i>Core</i>	<i>SAMO 14-2</i>											
N	72	76	76	77	78	78	78	78	78	78	78	
Min	<DL	60.4	7.3	26.3	1.9	0.2	34.7	38.0	0.3	0.5	0.3	
Max	31.7	91.2	25.0	196	12.2	0.5	128	187	7.1	13.9	2.7	
Mean	3.9	83.7	12.7	94.8	7.3	0.4	86.5	130	3.9	3.5	0.6	
SD	5.9	5.4	3.1	41.0	2.7	0.1	26.2	40.4	2.0	2.5	0.4	
<i>Core</i>	<i>SAMO 14-3</i>											
N	90	90	90	91	91	91	91	91	91	91	91	
Min	<DL	61.5	8.8	27.1	3.4	0.2	42.5	52.9	0.6	0.4	0.1	
Max	22.4	88.6	29.4	204	10.7	0.6	121	244	6.5	5.4	1.3	
Mean	4.0	82.6	13.4	93.1	6.9	0.4	81.5	139	3.3	2.0	0.5	
SD	4.7	5.1	3.4	46.6	1.8	0.1	19.5	43.3	1.5	1.1	0.3	
<i>Core</i>	<i>SAMO 18-4</i>											
N	36	36	36	36	36	36	36	36	36	36	36	
Min	0.6	76.3	9.6	82.2	7.0	0.4	90.6	105	4.2	0.9	0.1	
Max	12.4	85.2	16.0	214	10.2	0.5	127	161	6.8	2.0	0.6	
Mean	4.6	82.3	13.0	162	8.3	0.5	106	139	5.0	1.3	0.3	
SD	2.8	2.2	1.4	32.7	0.7	0.03	9.6	14.0	0.6	0.3	0.1	
<i>Background values</i>												
BC	4.3	82.0	13.8	133	8.4	0.5	95.3	154	4.5	2.6	0.5	
uBC	5.9	5.6	3.6	52.8	1.5	0.1	17.2	30.6	1.3	1.8	0.3	
BC <sub>M</sub>	–	–	–	–	7.8	–	–	–	–	–	–	
uBC <sub>M</sub>	–	–	–	–	2.5	–	–	–	–	–	–	
BC <sub>B</sub>	–	–	–	–	–	–	–	–	–	–	–	
TEL	–	–	–	–	–	–	–	–	–	–	–	
PEL	–	–	–	–	–	–	–	–	–	–	–	
	Ca	Sr	C <sub>org</sub>	C <sub>inorg</sub>	As	Co	Cr	Cu	Ni	Pb	V	Zn
<i>Core</i>	<i>SAMO 14-1</i>											
N	84	84	45	45	84	84	84	84	84	84	84	84
Min	1.8	254	0.9	0.2	37.4	<DL	12.9	18.2	7.2	<DL	50.6	50.5
Max	18.7	2246	6.5	6.0	236	25.5	92.2	34.3	32.7	47.6	169	172
Mean	7.8	623	2.7	2.2	92.7	13.4	36.7	26.0	20.7	15.3	115	114
SD	4.4	437	1.0	1.6	43.8	5.6	14.2	2.6	5.7	11.4	29.4	29.7
<i>Core</i>	<i>SAMO 14-2</i>											
N	78	78	41	41	78	78	78	78	78	78	78	78
Min	1.5	257	1.3	0.2	50.9	<DL	15.2	20.3	19.8	<DL	47.4	41.0
Max	18.5	2313	8.6	5.7	281	24.1	46.2	30.1	48.5	22.8	178	167
Mean	7.6	663	3.3	2.6	130	12.9	31.1	25.6	36.0	7.4	118	109



**Table 1** (continued)

	Ca	Sr	C <sub>org</sub>	C <sub>inorg</sub>	As	Co	Cr	Cu	Ni	Pb	V	Zn
SD	4.6	484	1.8	1.5	58.5	6.2	7.3	2.0	7.9	8.0	38.3	36.3
<i>Core</i>	<i>SAMO 14–3</i>											
N	91	91	47	47	91	91	91	91	91	91	91	91
Min	1.7	249	1.1	0.2	31.8	3.1	15.8	20.8	11.9	<DL	59.1	51.3
Max	16.7	2146	5.6	7.2	267	23.1	157	46.2	46.9	33.3	167	177
Mean	7.8	712	3.0	2.3	95.8	12.3	51.4	28.9	23.4	10.3	104	104
SD	4.0	463	1.0	1.6	44.9	4.4	27.9	4.1	6.4	9.2	24.9	27.4
<i>Core</i>	<i>SAMO 18–4</i>											
N	36	36	36	36	36	36	36	36	36	36	36	36
Min	1.7	264	1.2	0.3	52.9	12.9	28.5	23.3	19.6	26.8	129	117
Max	8.9	999	4.1	2.5	91.2	24.5	42.1	82.2	31.0	46.9	205	183
Mean	5.7	652	2.3	1.4	63.5	17.1	35.9	27.7	26.1	33.7	154	143
SD	1.7	169	0.6	0.5	8.6	2.9	3.1	9.4	2.7	5.4	18.8	16.1
<i>Background values</i>												
BC	5.9	430	2.3	1.6	88.9	15.4	44.9	27.4	29.1	14.5	127	122
uBC	3.4	141	0.7	1.1	38.5	4.2	22.8	3.6	8.9	9.7	26.3	26.5
BC <sub>M</sub>	–	–	–	–	83.2	13.6	34.9	26.6	24.9	18.2	116	117
uBC <sub>M</sub>	–	–	–	–	24.1	4.8	8.5	2.5	6.7	10.2	31.1	35.5
BC <sub>B</sub>	–	–	–	–	1.1	10.0	7–13	10–25	9.9	4–17	50	7–38
TEL	–	–	–	–	5.9	–	37.3	35.7	18.0	35.0	–	123
PEL	–	–	–	–	17.0	–	90.0	197	36.0	91.3	–	315

Sand, silt, clay, C<sub>org</sub>, C<sub>inorg</sub>, Al, Ti, Fe, and Ca are in %, magnetic susceptibility (MS) in 10<sup>-5</sup> SI, Mn in mg g<sup>-1</sup>, Rb, Zr, S, Sr, As, Co, Cr, Cu, Ni, Pb, V and Zn in µg g<sup>-1</sup>

BC background values from data for the pre-1900 period, uBC uncertainty of BC (1 σ);

BC<sub>M</sub>=background values derived from Matschullat et al. (2000); uBC<sub>M</sub>=uncertainty of BC<sub>M</sub> (from cores SAMO14-1, 14-2 and 14-3; see explanation in the text)

BC<sub>B</sub>=background level, TEL=threshold effect level, and PEL=probable effect level for lake sediments from Buchman (2008)

<DL=below limit of detection (sand: 0.5%, Co: 3 µg g<sup>-1</sup>, and Pb: 1 µg g<sup>-1</sup>)

### Trace element provenance

Because anomalous trace element concentrations are not always the result of anthropogenic contamination, and can instead reflect differences in sediment sources (Loring and Rantala 1992), factor analysis (FA) was used to infer the provenance of the trace elements, especially As, which showed the highest enrichment factors in the deep cores (Fig. 5). Bartlett’s test of sphericity yielded a *p*-value < 0.05, confirming that the dataset has significant correlations among at least some of the variables; and the KMO test provided an overall MSA = 0.88 and values > 0.5 for all variables (Table 2), corroborating the suitability of the database for FA.

Three factors (eigenvalues > 1.0) explained 75% of the dataset variance (Table 2, Fig. 6). Factor 1 (F1,

54% explained variance—ev) represents sedimentary matter; it included as significant variables Ca, C<sub>inorg</sub>, C<sub>org</sub>, Sr, As, S and silt with negative values, and Fe, Rb, Ti, Zr, and Al (detrital proxies; Sageman and Lyons 2004) and the trace elements Zn, Pb, Co, and V with positive values. Factor 2 (F2, ev = 12%) denotes grain size variability; it included silt and clay with negative loadings and sand with positive loading. Factor 3 (F3, ev = 9%) represents diagenetic effects; it included Mn with positive loadings, as well as Cu and Cr with negative loadings.

In the FA biplot of F1 and F2, which explained most of the dataset variance, the sections of cores SAMO 14–1, SAMO 14–2, and SAMO 14–3 are scattered throughout both factors, although most samples from the post-1950 period are distributed on the negative side of factor 1 (quadrants III and IV); whereas

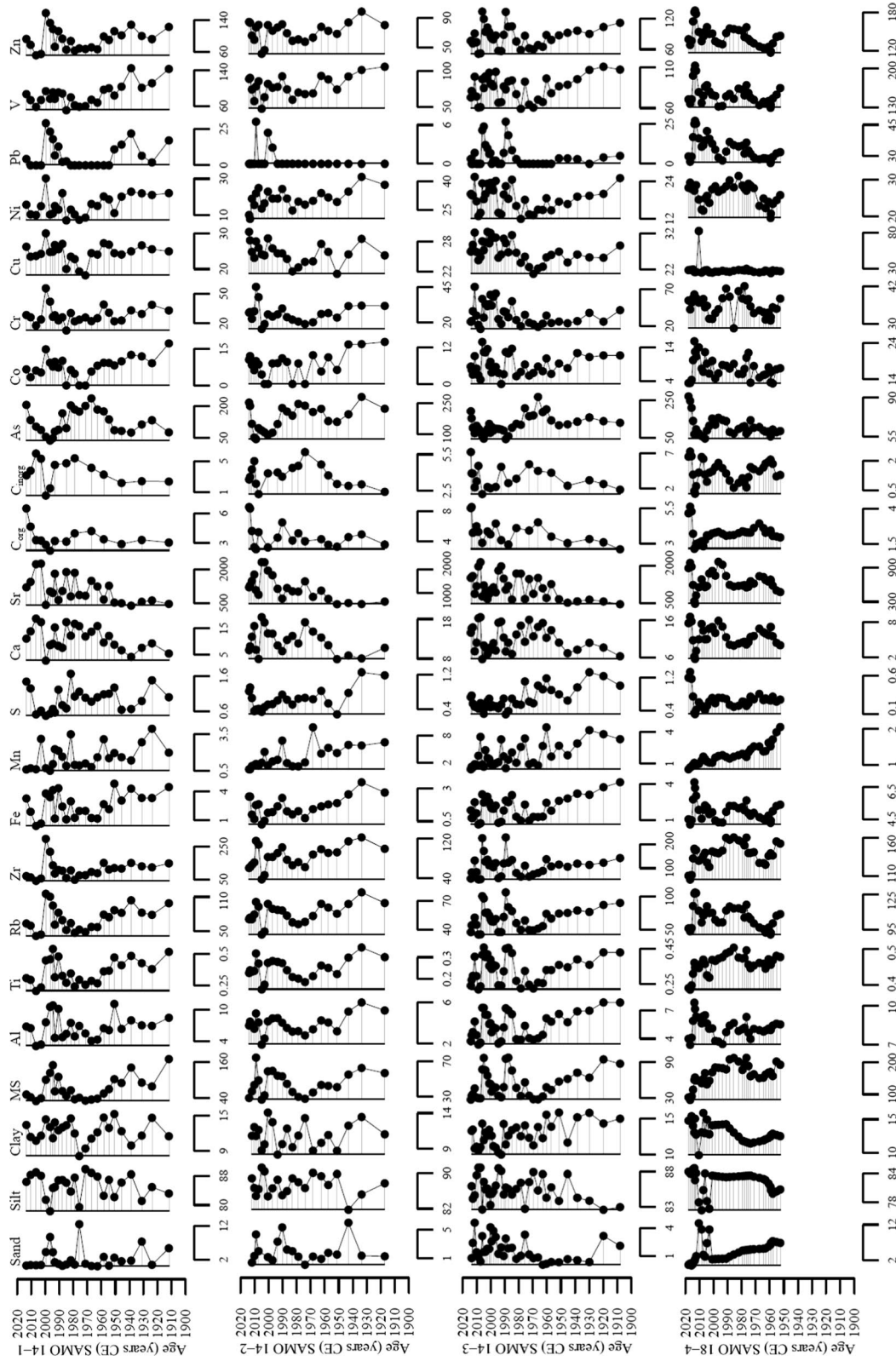
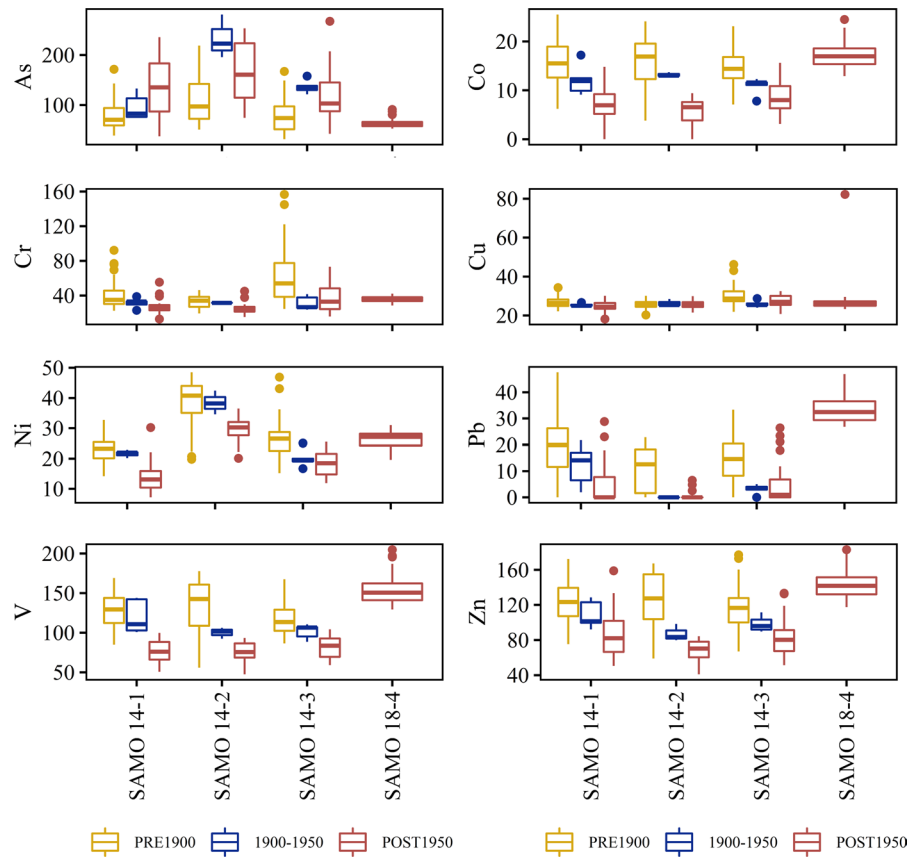


**Fig. 3** Temporal profiles of grain size distribution (%), magnetic susceptibility ( $\times 10^{-5}$  SI), and element concentrations in sediment cores from Santa María del Oro Lake, Mexico. Units: Al, Ca and Ti (%), Rb, Zr, Sr and trace elements ( $\mu\text{g g}^{-1}$ )

**Fig. 4** Boxplot of trace element concentrations by periods, in sediments from Santa María del Oro Lake, NW Mexico. Trace element concentrations are in  $\mu\text{g g}^{-1}$



almost all sections of core SAMO 18–4 were grouped on the positive side of both factors (quadrants I and II).

In the FA solution it was noted that: (1) silt percentages have cross-loadings with similar significant values (-0.56 in F1, and -0.60 in F2), which indicates that silt contributes to explain two separate concepts (Hair et al. 2014), and (2) despite the fact that Ni had an acceptable MSA (0.66, Table 2), it showed a low communality (0.14) and did not have significant loadings in any factor, which indicated that the variance shared by Ni concentrations with other variables is low, so Ni variability is not accounted for by the FA solution (Hair et al. 2014).

Trace element concentrations in soils

The trace element concentrations in soils collected in the SAMO surroundings (ESM Table S1) fell mostly within the range of values observed in the SAMO sediment cores, except for As, which were

considerably lower than the As concentrations in the deep cores.

Discussion

The element concentration ranges observed in SAMO are comparable to those reported for other lakes (Table 3), including (i) non-contaminated environments (e.g. Cr and Ni in Bafa Lake, Turkey (Manav et al. 2016) or Zn in Popradske Lake, Slovakia (Reczýnski et al. 2020)), or (ii) contaminated environments (e.g. As in Paulina Lake, USA (Lefkowitz et al 2017), Co in Bizerte Lagoon, Tunisia (Mna et al. 2017), Cu, Pb and Zn in Uru Uru Lake, Bolivia (Tapia and Audry 2013)). Some concentrations reported for non-contaminated environments are similar to those reported for contaminated environments (Table 3), because trace element concentrations can be influenced by sediment geochemical properties (e.g. grain size, carbonates, or organic matter

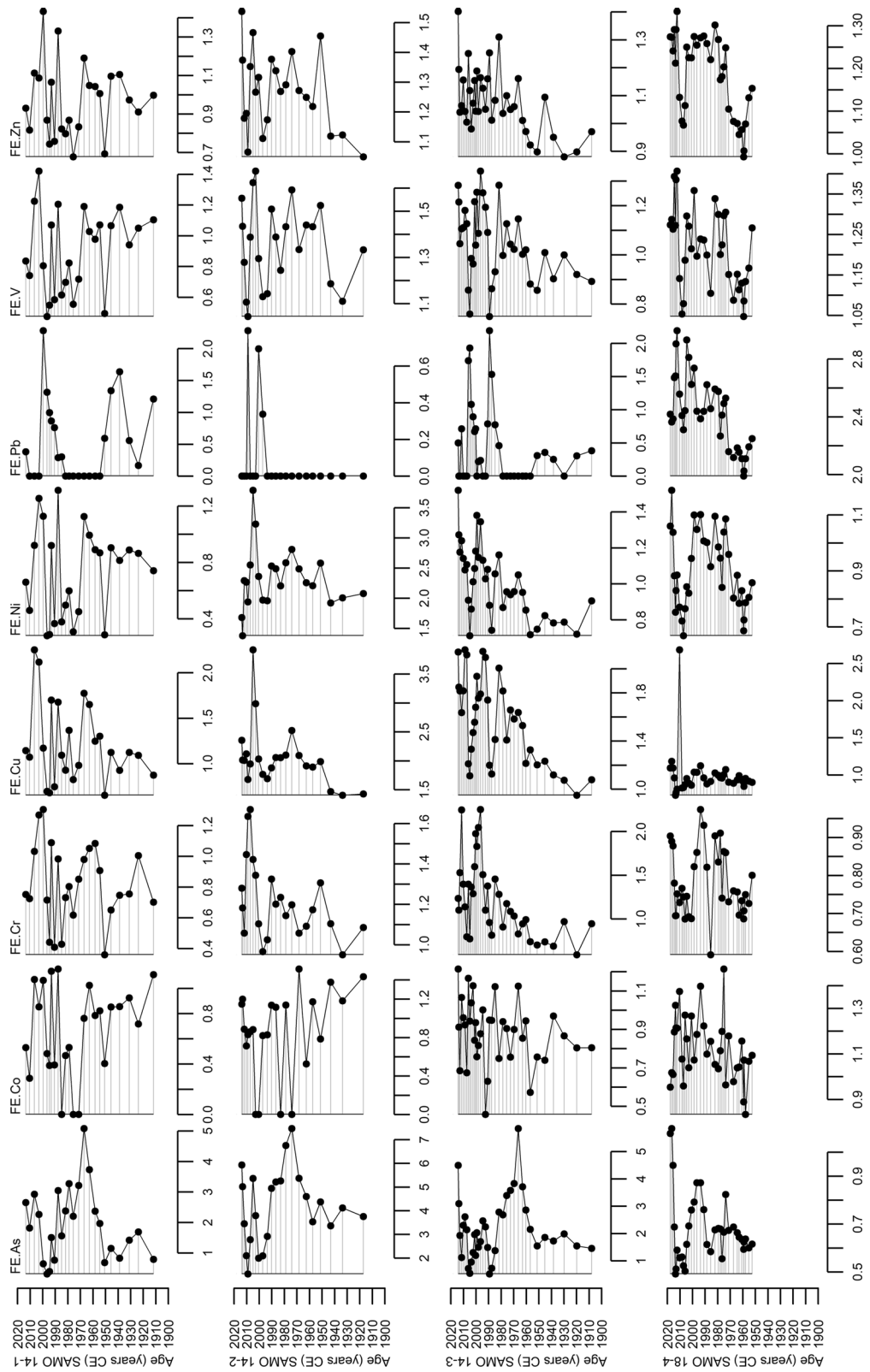


**Fig. 5** Temporal profiles of trace element enrichment factors in sediment cores from Santa María del Oro Lake, NW Mexico

**Table 2** Factor analysis for elemental composition in sediment cores from Santa María del Oro Lake NW Mexico

Variable	MSA	Factor1	Factor2	Factor3	Communality
Ca	0.82	-0.96	-0.03	-0.04	0.92
C <sub>inorg</sub>	0.95	-0.94	0.02	0.07	0.89
C <sub>org</sub>	0.91	-0.91	-0.08	-0.14	0.85
Fe	0.90	0.90	-0.09	0.27	0.90
Rb	0.92	0.90	-0.34	0.00	0.93
Zn	0.91	0.90	-0.35	-0.06	0.94
Ti	0.93	0.87	-0.18	-0.14	0.81
Sr	0.92	-0.86	-0.08	-0.31	0.84
Zr	0.88	0.85	-0.07	-0.11	0.74
Pb	0.84	0.85	0.19	-0.14	0.78
Al	0.86	0.84	-0.27	0.14	0.79
Co	0.95	0.83	-0.13	0.09	0.72
V	0.93	0.81	-0.35	0.05	0.78
As	0.89	-0.78	-0.42	0.26	0.85
S	0.67	-0.71	-0.28	0.33	0.70
Sand	0.51	0.20	0.85	-0.06	0.76
Clay	0.71	-0.10	-0.72	-0.10	0.54
Silt	0.80	-0.56	-0.60	-0.30	0.77
Cu	0.64	-0.26	-0.33	-0.75	0.75
Mn	0.67	-0.38	-0.10	0.67	0.60
Cr	0.51	0.23	0.26	-0.58	0.45
Ni	0.66	0.30	-0.22	0.04	0.14
Explained variance (%)		54	12	9	

MSA measure of sampling adequacy from the Kaiser–Meyer–Olkin (KMO) test; overall value=0.88. Significant elements (in bold) have loadings >0.55

concentrations; Horowitz 1985) and are also strongly dependent on the mineralogical composition of catchment sediments, which mostly defines the background concentrations.

The background concentrations of trace elements in SAMO were estimated from the pre-1900 data in the deep cores, which were not available for SAMO 18–4. Although a few significant differences were observed for some element concentrations among the cores, we considered that an overall interval from the three deep cores better represents the concentrations in the lake. Between the sixteenth and eighteenth centuries, during the Spanish occupation of Mexico, three small gold mines (*reales*) operated within the current territory of Santa María del Oro Municipality, although those mining centers were abandoned after the Mexican War of Independence in 1810 (Gómez-Cancino 2016; INAFED 2010). There is no information on the impacts of those mining centers on SAMO; thus, the background values reported here may not represent natural values, but serve as a baseline to evaluate trace element contamination over the past century. The background values of Co, Cu, and Pb were comparable to background values for freshwater sediments in the NOAA Screening Quick Reference Tables (Buchman 2008), although higher values were observed for Cr, Ni, V, and Zn (~3 times higher), and As (~81 times higher).

Indeed, As, Cr, and Ni background concentrations in SAMO are high, and according to the PEL benchmark, these concentrations could be harmful to benthic biota. The high background values in SAMO could be related to the volcanic lithology and the

**Fig. 6** Factor analysis biplot for geochemical variables and trace element concentrations in sediment cores from Santa Maria del Oro Lake, NW Mexico. Biplot quadrants are indicated by Roman numerals

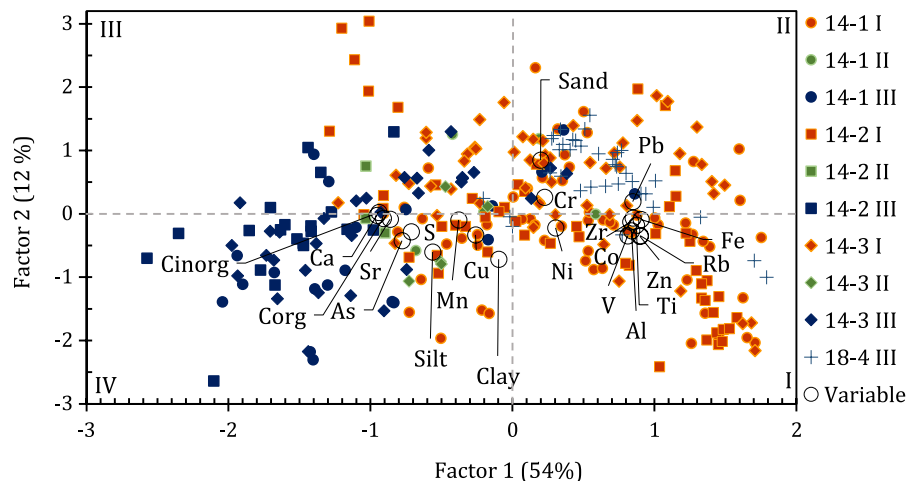


**Table 3** Trace element concentrations in lakes around the world (concentrations are in  $\mu\text{g g}^{-1}$ )

Study site	As	Co	Cr	Cu	Ni	Pb	V	Zn	Status
Santa María del Oro Lake <sup>1</sup>	31.8–280.8	3.1–25.5	12.9–156.7	18.2–82.2	7.2–48.5	1.2–47.6	47.4–204.9	41.0–182.9	NC
Espejo de Lirios Lake, Mexico <sup>2</sup>	NA	38.8–67.1	42.9–67.1	20.5–30.8	39.8–61.1	53.8–116.0	37.7–61.1	102–148	C
Santa Elena Lake, Mexico <sup>3</sup>	5.0–8.2	NA	42.3–53.4	8.7–15.0	NA	24.6–31.7	63.6–90.7	50.1–75.1	NC
Chapala Lake, Mexico <sup>3</sup>	6.0–9.4	NA	43.7–57.6	23.4–28.3	NA	18.8–31.0	86.2–111	85.1–198	C
El Sol Lake, Mexico <sup>4</sup>	2.1–6.3	7.7–15.2	35.6–54.1	35.6–63.5	14–22	33.6–142	68.0–100.9	96.3–156	C
La Luna, Mexico <sup>4</sup>	1.6–7.9	8.7–32.1	36.8–53.0	30.8–67.9	14–26	24.2–172	50.9–99.2	88.9–184	C
Lago Verde, Mexico <sup>5</sup>	NA	NA	NA	54.3–169.5	NA	2.1–65.5	NA	35.3–143.4	
Holiday Lake, EUA <sup>6</sup>	17.4	NA	26.6	86.6	NA	23.7	NA	88.7	C
Germantown Lake, EUA <sup>6</sup>	28.3	NA	25.3	46.9	NA	26.0	NA	88.9	C
Bear Creek Lake, EUA <sup>6</sup>	27.7	NA	25.4	31.5	NA	15.9	NA	90.2	C
Chesdin Lake, EUA <sup>6</sup>	18.1	NA	24.2	50.4	NA	25.0	NA	88.8	C
East Lake, EUA <sup>7</sup>	22–34	4–6	6–14	5–15	4–6	0–3	62–88	11–24	C
Paulina Lake, EUA <sup>7</sup>	33–247	16–67	0–8	1–8	41–144	0–8	54–138	21–63	C
Wielki Staw Lake, Poland <sup>8</sup>	NA	NA	NA	3.4–19.1	NA	4.9–75.0	<0.4–31.6	11.7–55.0	C
Lago Smreczynski, Poland <sup>9</sup>	NA	NA	12.3–37.4	18.4–43.6	NA	146.1–352.6	NA	133.0–537.8	C
Lago Popradske, Slovakia <sup>9</sup>	NA	NA	9.9–18.5	8.6–22.1	NA	13.7–18.2	NA	126.1–190.9	NC
Bafa Lake, Turkey <sup>10</sup>	NA	NA	214–288	NA	297–460	8.3–19.1	NA	67.5–89.9	NC
Erhai Lake, China <sup>11</sup>	NA	NA	93–179	56–117	52–92	53–75	NA	120–164	C
Rewalsar Lake, India <sup>12</sup>	NA	10.5–16.3	64.7–165.0	24.6–97.0	23.3–50.0	19.7–29.0	NA	84–116	C
Hussian Sagar Lake, India <sup>13</sup>	8.4–20.8	8.3–15.1	67.2–105.8	52.6–137.5	26.6–70.6	50.7–134.8	NA	96.7–441.9	C
Willsmere Billa-bong, Australia <sup>14</sup>	2.5–7.0	NA	33.0–37.0	9.0–14.0	17–23	13.0–17.0	NA	30.0–64.0	NC
Bizerte Lagoon, Tunisia <sup>15</sup>	NA	17.0–24.0	155–210	0.3–22.0	52–88	100–190	NA	163–257	C
Dianchi Lake, China <sup>16</sup>	21.5–64.4	NA	57.2–113	57.3–114	33–59.8	44.1–105	NA	132–606	C
Uru Uru Lake, Bolivia (north) <sup>17</sup>	37–76	NA	NA	43–81	NA	33–60	NA	107–183	C

C contaminated, NC not contaminated, NA not available

Data source: This study<sup>1</sup>, Ruiz-Fernández et al. (2004)<sup>2</sup>, Ontiveros et al. (2014)<sup>3</sup>, Ontiveros-Cuadras et al. (2014)<sup>3</sup>, Hernández-Rivera (2018)<sup>4</sup>, Hernández-Rivera (2018)<sup>4</sup>, Ruiz-Fernández et al. (2007)<sup>5</sup>, Coxon et al. (2016)<sup>6</sup>, Lefkowitz et al. (2017)<sup>7</sup>, Malkiewicz et al. (2016)<sup>8</sup>, Reczynski et al. (2020)<sup>9</sup>, Manav et al. (2016)<sup>10</sup>, Li et al. (2017)<sup>11</sup>, Meena et al. (2017)<sup>12</sup>, Ayyanar and Thatikonda (2020)<sup>13</sup>, Lintern et al. (2016)<sup>14</sup>, Mna et al. (2017)<sup>15</sup>, Li et al. (2020)<sup>16</sup>, Tapia and Audry (2013)<sup>17</sup>

presence of mineralized zones in the catchment. Concentrations of As in volcanic rocks are generally low (e.g. 3.2–5.4  $\mu\text{g g}^{-1}$  for rhyolite, and 0.18–113  $\mu\text{g g}^{-1}$  for basalt, the predominant rock types in the SAMO catchment), although As can be enriched in sulfide mineral veins in volcanic rocks (Smedley and Kinniburgh 2002).

Most trace element concentrations showed narrow variations within the past 100 years (Fig. 3). The enrichment factors in SAMO cores (Fig. 5) were usually low, ranging from no enrichment ( $\text{EF} < 2$ ) by Co, V and Zn, to mostly minor enrichment by Cr, Cu, Ni and Pb in at least one of the deep cores, but only by Pb in SAMO 18–4. This means that, from the inorganic geochemical point of view, SAMO is still a well-preserved environment, barely affected by human impact during the past century—but not pristine, since the human imprint is everywhere and truly pristine environments are essentially nonexistent (Stahn et al. 2017). The exception was As, for which  $\text{EF} > 2$  was observed since the early 1900s in SAMO 14–2 and, during the post-1950 period, the EF reached values as high as  $\sim 7$  (moderately severe enrichment) in the deep cores (Fig. 5).

Major natural sources of As in lakes include the weathering of As-bearing minerals such as sulfides and sulfo-salts (Schaufelberger 1994) and groundwaters enriched with geogenic As, i.e. associated with mineral deposits, volcanic or hydrothermal processes. Residues from diverse anthropic activities, such as mining of metal ores, use of wood preservatives, pesticides, fertilizers, and sewage discharge, among others (Camacho et al. 2011) can be responsible for arsenic contamination in surface water and groundwater. Regarding As particulate transport, neither the sediment nor soil data support that the As enrichment has an anthropic origin, since: (a) As concentrations in SAMO 18–4, collected closer to the shoreline, and thus more influenced by anthropogenic activities, were comparable to background As concentrations ( $89.9 \pm 40.2 \mu\text{g g}^{-1}$ ) in the lake, and (b) As concentrations in the soils collected around the lake (ESM Table S1), with a mean value of  $39.7 \pm 54.0 \mu\text{g g}^{-1}$ , were lower than those observed in the sediment cores, and in only two of the soil samples collected in the southern part of the lake, As concentrations (S-01:  $136 \mu\text{g g}^{-1}$  and S-02:  $146 \mu\text{g g}^{-1}$ ) were comparable to the background values in SAMO cores.

Concentrations of As in stream sediments from mineralized areas in the SAMO surroundings (CRM 1996) are considerably higher ( $770\text{--}1043 \mu\text{g g}^{-1}$ ; Table EMS S1). Thus, underground transfer of As to SAMO may be possible, but no information on As concentrations in groundwater is yet available to support this surmise.

#### Trace element provenance

According to the factor analysis, F1 (sedimentary matter,  $\text{ev} = 54\%$ ) indicated that autochthonous production and terrigenous input are the main processes that regulate trace element composition in SAMO sediments. The terrigenous input resulting from catchment erosion, as indicated by the lithogenic elements Fe, Al, Ti, Rb, and Zr in the negative-loading assemblage, is the main source of Co, Pb, V, and Zn, as these elements can be firmly bound in mineral lattices (Boyle et al. 2002); the scavenging of As by endogenic/ authigenic phases (carbonates, organic matter, and sulfides), however, largely influences the accumulation of As in the sediments, as indicated by the positive-loading assemblage (Ca, Sr,  $\text{C}_{\text{org}}$ ,  $\text{C}_{\text{inorg}}$ , As, S, and silt).

The depth profile of factor scores (Fig. 7, Factor 1) showed that alternation between the two processes is more relevant for the deep cores, since along core SAMO 18–4, which covers only the post-1950 period, the factor scores are mostly positive, indicating the stronger influence of terrigenous input on the trace element distribution at the shallowest sampling location. The distribution of the core sections in the FA biplot (Fig. 6) reflected the main influence of land sources of Pb on SAMO 18–4, which showed the highest Pb concentrations among the cores (Fig. 4), accounting for Pb enrichment ( $\text{EF} > 2$ , Fig. 5). This minor Pb contamination might be caused by (i) long-distance transport of Pb deposited on catchment soils and transported to the lake by runoff (Rose et al. 2012), and (ii) human activities near the lake shore, which may include the use of household products such as leaded paint, solder, wood finishes, shot and bullets, jewelry, leaded ceramic and crystal containers for food and beverages, and improper waste management (e.g. disposal of electronic waste and lead batteries, and open burning of residues) (Laquatra 2014; ATSDR 2019). Domestic and agricultural (sugar cane) waste burning is a known issue in Santa María

del Oro Municipality, which also produces recurrent forest fires in the surroundings (SEDATU 2013). Open burning of waste can produce emissions of a variety of heavy metals, including Pb, through gaseous emissions and fly- and bottom-ash, creating the potential for further air, water, and soil contamination (Cogut 2016).

Accumulation of carbonates (represented by the grouping of Ca, Sr,  $C_{inorg}$ ) in the deep cores seems to counterbalance that of trace elements supplied from catchment runoff. Silt is included in the positive-loading assemblage of F1 (Table 2), likely because most carbonate deposition occurs as mud-sized material (Gierlowski-Kordesch 2010). Despite the small grain size, generally associated with a higher capacity to concentrate trace elements, carbonate minerals contain considerably lower trace element concentrations than do aluminosilicates (Veizer 1983), and together

with other assumed non-trace element-bearing materials (e.g. quartz and coarse-grained materials), are often considered diluents of trace element concentrations in sediments (Horowitz 1985). This dilution process is confirmed by the opposite concentration trends (Fig. 3) and loading signs (Table 2) between Ca and most trace element concentrations (Co, Cr, Ni, Pb, V, Zn).

Higher accumulation of carbonates was identified during the post-1950 period in all cores (relatively high Ca,  $C_{inorg}$ , and Sr concentrations in Fig. 3), notably in the deep cores (Fig. 6). Carbonate deposition may be induced by water-borne clastic input, eolian supply, concentration through evaporation, and biogenic activity (Gierlowski-Kordesch 2010). Given the opposite loading signs of carbonate and detrital indicators in F1, the clastic origin of carbonates is unlikely. Carbonate precipitation in SAMO may be

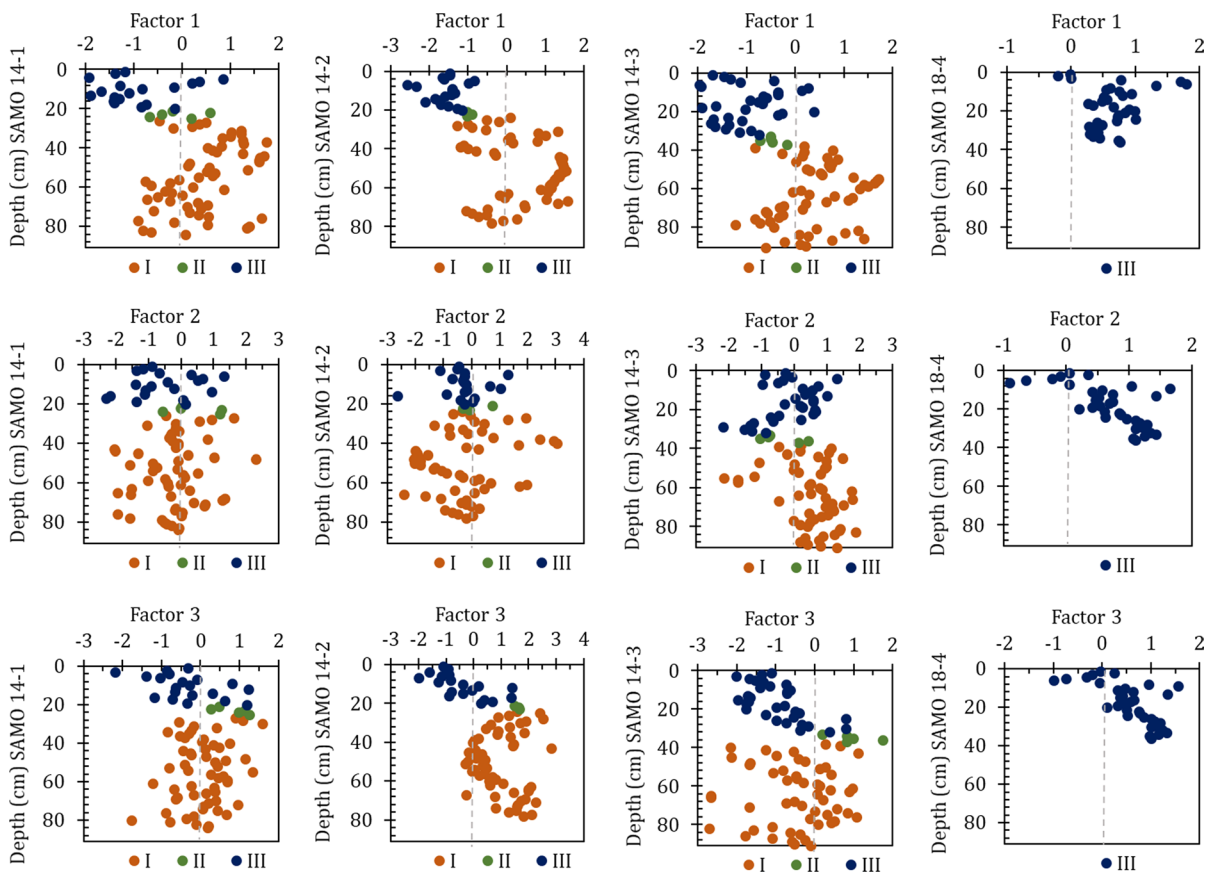


**Fig. 7** Depth profile of factor scores, from the factor analysis for geochemical variables and trace element concentrations in sediment cores from Santa Maria del Oro Lake, NW Mexico



influenced by cyanobacterial blooms after turnover (Caballero et al. 2013; Bustillos et al. 2020), as they are known to be responsible for large-scale precipitation of  $\text{CaCO}_3$ , together with organic compounds (Kamennaya et al. 2012). The temporal changes in carbonate production can be related to cyclic climate patterns (humidity/aridity and temperature) that may promote algae productivity and carbonate precipitation by concentration (Gierlowski-Kordesch 2010). A previous study of sediments accumulated within the past 2000 years in SAMO (Rodríguez-Ramírez et al. 2015) attributed increased carbonate deposition to low water levels, owing to lower rainfall and higher evaporation rates.

The association of As with the negative-loading assemblage is explained by biogeochemical processes, including carbonate precipitation (indicated by the grouping of Ca,  $\text{C}_{\text{inorg}}$ , and Sr), as well as organic matter complexation and trapping in authigenic sulfide minerals, as per the grouping of  $\text{C}_{\text{org}}$  and S. Primary production causes an increase in pH and precipitation of calcium carbonate, the removal of trace metals by their incorporation into algal tissues and new mineral phases, and provides active surfaces for adsorption (Salomons and Förstner 1984). In aqueous environments, the most abundant inorganic As species are arsenate (As(V)) and arsenite (As(III)), and the mobility of these species is influenced by pH and the redox potential, as well as the presence of adsorbents, such as Fe- Mn- and Al-oxides, sulfide minerals, phyllosilicates (e.g. micas and clays), carbonates and organic matter (Magalhães 2002; Neff 2002; Panagiotaras and Nikolopoulos 2015). Although arsenate is favored in oxic conditions and arsenite in anoxic conditions, both As species are found in reduced and oxidized settings (Nicomel et al. 2015). Under oxic conditions As is mostly adsorbed to metal oxides, whereas in reducing conditions, metal oxide dissolution releases As and it can be trapped in authigenic sulfide minerals (Costagliola et al. 2013), calcite (either incorporated in the calcite crystal lattice or adsorbed at the mineral surface; Renard et al. 2015), or can complex with natural organic matter (Catrouillet et al. 2016), whose diverse functional groups (e.g. carboxylic, amino, sulfhydryl, hydroxyl) are efficient geochemical traps for As, under both oxic and reducing conditions (Zhu et al. 2017).

According to the FA biplot (Fig. 6, quadrant IV), carbonate and As accumulation are more relevant in the deep cores than in the shallow one, especially during the post-1950 period, when minor to moderately severe enrichments were observed (Fig. 5). The deep cores were collected below the oxycline, where anoxic conditions are almost permanent (Caballero et al. 2013), and reducing conditions would favor the availability of effective scavengers for As, such as inorganic sulfides, Mn(II)-bearing carbonates (rhodochrosite,  $\text{MnCO}_3$ ) (Johnson et al. 2016) and the sulfur-enrichment of organic matter (Urban et al. 1999).

As indicated by F2, the grain size variability in SAMO sediments refers mostly to the sand and clay percentages in the sediments (highest loadings in F2), which are the less represented in the cores (all cores have >60% of silt; Table 1). These variations are much more intermittent in the deep cores than in the shallow one (Fig. 7, Factor 2); however, their influence on the accumulation of trace elements seems to be minimal, as none of them have significant loadings in this factor.

According to F3, the variation of Cr and Cu concentrations in the sediments is most likely driven by diagenetic processes, as suggested by the significant loading of the redox-sensitive element Mn in this factor. This would imply that the profiles of the three elements are likely influenced by post-depositional migration and reprecipitation as a consequence of the seasonal cycle of lake stratification. Mn and Fe undergo oxidation and reduction as lakes periodically overturn and stagnate; in the oxidized state, both of them are insoluble and precipitate as Mn and Fe oxides, carrying adsorbed ions to the sediments, whereas under anoxic conditions they solubilize, release the adsorbed ions, which diffuse upward and precipitate as oxides in the oxidizing part of the sediment sequence or are released to the water column (Balistrieri et al. 1992; Howard and Chisholm 1975); however, the oxidation of Mn is much slower and the reductive dissolution of Mn oxyhydroxides faster, than that of Fe (Davison 1993). The contrasting trends of Cr and Cu in comparison to Mn (Fig. 3; opposite loading signs in F3, Table 2) can be explained by the different effects of redox processes on these elements. Under reducing conditions, whereas Mn solubilizes, Cr tends to precipitate as  $\text{Cr}(\text{OH})_3$  or be adsorbed onto mineral phases, such as Al and Fe oxides, calcite, and organic matter coatings, whereas

under oxidizing conditions Mn precipitates and Cr is generally soluble and rarely forms precipitates (Murray et al. 1983; Gorny et al. 2016). Regarding Cu, it is generally associated with clay mineral fractions, especially those rich in coatings that contain organic carbon and oxides of Fe and Mn (Callender 2003), whereas under reducing conditions, Cu is released to solution and diffuses downward within the sediments, where it can be fixed by coprecipitation with sulfide phases or by incorporation into authigenic clay minerals (Pedersen et al. 1986). Variations in the depth profiles (Fig. 7, Factor 3) in the shallow core, which covers only the post-1950 period, are minimal in comparison with the deep cores, which seem to be more affected by diagenetic processes, owing to the greater depth and almost permanent anoxic conditions that prevail in the hypolimnion.

The FA was not useful to explain the variability of Ni in the cores, because the variance shared with the other variables in the analysis was low. This might be because Ni is less particle-reactive than other elements analyzed, such as Pb, Co, Cu, or Zn (Balls et al. 1989; Burton et al. 1993). The dominant form of Ni in natural freshwaters is soluble  $\text{Ni}^{2+}$  (Bin et al. 2018) and the free ionic form  $\text{Ni}^{2+}$  is stable over a range of redox conditions. Nickel can form soluble complexes with inorganic and organic ligands, and/or is associated with suspended mineral colloids. Thus, geogenic Ni can be mobilized to a considerable amount, depending on both the redox potential and pH of the environment (Rinklebe and Shaheen 2017).

In summary, the main provenance of the trace elements in the cores is terrigenous for Co, Pb, V, and Zn, and hydrogenous for As (owing to sorption or coprecipitation with endogenic/authigenic phases) and Cu and Cr (diagenetic reactions). Climate change can affect trace element deposition in lakes through multiple processes, including variations in temperature and rainfall rates, which could alter mixing and stratification patterns and reduce lake water levels, which may intensify heavy metal cycling in lake sediments (Zhang et al. 2018). According to data from the Cerro Blanco meteorological station, located ~5 km NW of SAMO, precipitation decreased significantly between 1960 and 2010 (Ruiz-Fernández et al. 2022). Reduced rainfall would likely have favored increased lake water evaporation and endogenic carbonate precipitation, and this process may have contributed to high As enrichment in the deep cores. Since

increasing drought periods are foreseen in the area, and SAMO water extraction might also contribute to lowered lake water levels (PO 2003), As enrichment could increase in the future.

## Conclusions

Temporal changes in environmental conditions at crater lake Santa María del Oro (NW Mexico) were evaluated through analysis of trace element concentrations (As, Co, Cr, Cu, Ni, Pb, V, and Zn) in four  $^{210}\text{Pb}$ -dated sediment cores. Background trace element concentrations were established from lake sediments accumulated before the 1900s and can serve as a baseline for future studies and lake management programs.

As, Cr and Ni concentrations were found to be naturally high, and enrichment factors of most trace elements implied negligible recent anthropogenic contamination. Nonetheless, moderately severe As enrichment was observed in the deep lake cores, attributed to biogeochemical processes, notably carbonate precipitation, likely driven by climate variability. According to international benchmarks, As concentrations could be deleterious to benthic biota and to humans, through fish consumption, for which specific studies on As toxicity are recommended.

Considering that drought conditions might promote further As enrichment, evaluation of As concentrations in water and fish, and surveillance of the lake water level (owing to water extraction and droughts) is also advisable. So far, anthropogenic activities in the proximity of the lake within the past 100 years have had a small impact on the environmental quality of the lake, at least regarding trace element contamination. However, anthropogenic activities in the catchment should be monitored to preserve the conditions of this valuable water resource.

**Acknowledgements** This work was supported by the grants UNAM DGAPA-PAPIIT/104718 and Newton Mobility Grant NMG\R2\170126. Thanks are due to Donají Maribel Hernández Rivera, Melisa Sánchez, Carlos Suárez and León Felipe Álvarez for technical assistance. The authors sincerely appreciate all valuable comments and suggestions from Antonio Martínez Cortizas, who helped us improve the quality of the manuscript.

## References

- Algül F, Beyhan M (2020) Concentrations and sources of heavy metals in shallow sediments in Lake Bafa, Turkey. *Sci Rep* 10:1–12
- ATSDR (2019) Lead toxicity. Where is lead found? Environmental Health and Medicine Education. Agency for Toxic Substances and Disease Registry. <https://www.atsdr.cdc.gov/csem/csem.asp?csem=34&po=5>. Accessed 11 Sept 2020
- AWG (2019) Results of binding vote by AWG. Working Group on the 'Anthropocene'. <http://quaternary.stratigraphy.org/working-groups/anthropocene/> Accessed 23 April 2020
- Ayyanar A, Thatikonda S (2020) Distribution and ecological risks of heavy metals in Lake Hussain Sagar, India. *Acta Geochim* 39:255–270
- Balistrieri LS, Murray JW, Paul B (1992) The cycling of iron and manganese in the water column of Lake Sammamish, Washington. *Limno Oceanogr* 37:510–528
- Balls PW (1989) The partition of trace metals between dissolved and particulate phases in European coastal waters: a compilation of field data and comparison with laboratory studies. *Neth J Sea Res* 23:7–14
- Bianchi TS (2007) *Biogeochemistry of Estuaries*. Oxford University Press, New York
- Binet MT, Adams MS, Gissi F, Golding LA, Schlekot CE, Garman ER, Merrington G, Stauber JL (2018) Toxicity of nickel to tropical freshwater and sediment biota: a critical literature review and gap analysis. *Environ Toxicol Chem* 37:293–317
- Birch GF (2017) Determination of sediment metal background concentrations and enrichment in marine environments. *Sci Total Environ* 580:813–831
- Birch GF, Davies KI (2003) A scheme for assessing human impact and sediment quality in coastal waterways. In: Woodroffe CD, Furness RA (eds) *Proceedings of the Coastal GIS Conference*. Wollongong Papers on Maritime Policy 14, Australia pp 7–8
- Boyle JF (2002) Inorganic geochemical methods in palaeolimnology. In: Last WM, Smol JP (eds) *Tracking environmental change using lake sediments*. Developments in paleoenvironmental research. Springer, Dordrecht, pp 83–141
- Buat-Menard P, Chesselet R (1979) Variable influence of the atmospheric flux on the trace metal chemistry of oceanic suspended matter. *Earth Planet Sci Lett* 42:398–411
- Buchman MF (2008) NOAA screening quick reference tables, NOAA OR&R Report 08–1, Seattle WA, Office of Response and Restoration Division, National Oceanic and Atmospheric Administration, p 34. <https://repository.library.noaa.gov>
- Burton JD, Althaus M, Millward GE, Morris AW, Statham PJ, Tappin AD, Turner A, Balls P, Stebbing ARD (1993) Processes influencing the fate of trace metals in the North Sea. *Philos Trans R Soc Lond A* 343:557–568
- Bustillos-Guzmán JJ, Turner A, Hernández-Almeida OU, Band-Schmidt CJ, Romero-Bañuelos CA, Hernández-Sandoval FE, Núñez-Vázquez EJ, Palomino-Hermosillo YA (2020) Presence of cyanotoxins in a Mexican subtropical monomictic crater Lake. *Appl Sci* 10:1–5
- Caballero M, Rodríguez A, Vilaclara G, Ortega B, Roy P, Lozano S (2013) Hydrochemistry, ostracods and diatoms in a deep, tropical, crater lake in Western Mexico. *J Limnol* 72:512–523
- Callender E (2003) Heavy metals in the environment—historical trends. In: Holland HD, Turekian KK (eds) *Treatise on geochemistry*, vol 9. Elsevier, New York, pp 68–105
- Camacho LM, Gutiérrez M, Alarcón-Herrera MT, Villalba ML, Deng S (2011) Occurrence and treatment of arsenic in groundwater and soil in northern Mexico and southwestern USA. *Chemosphere* 83:211–225
- Cardoso-Mohedano JG, Sanchez-Cabeza JA, Ruiz-Fernández AC, Pérez-Bernal LH, Lima-Rego J, Giral S (2019) Fast deep water warming of a subtropical crater lake. *Sci Total Environ* 691:1353–1361
- Catrouillet C, Davranche M, Dia A, Bouhnik Le Coz M, Demangeat E, Gruau G (2016) Does As(III) interact with Fe(II), Fe(III) and organic matter through ternary complexes? *J Colloid Interface Sci* 470:153–161
- Cogut A (2016) Open burning of waste: a global health disaster. R20 Regions of climate action. [https://regions20.org/wp-content/uploads/2016/08/OPEN-BURNING-OF-WASTE-A-GLOBAL-HEALTH-DISASTER\\_R20-Reseach-Paper\\_Final\\_29.05.2017.pdf](https://regions20.org/wp-content/uploads/2016/08/OPEN-BURNING-OF-WASTE-A-GLOBAL-HEALTH-DISASTER_R20-Reseach-Paper_Final_29.05.2017.pdf) Accessed 11 Sept 2020
- Costagliola P, Bardelli F, Benvenuti M, Di Benedetto F, Lattanzi P, Romanelli M, Paolieri M, Rimondi V, Vaggelli G (2013) Arsenic-bearing calcite in natural travertines: evidence from sequential extraction,  $\mu$ XAS, and  $\mu$ XRF. *Environ Sci Technol* 47:6231–6238
- Coxon T, Odhiambo B, Giancarlo L (2016) The impact of urban expansion and agricultural legacies on trace metal accumulation in fluvial and lacustrine sediments of the lower Chesapeake Bay basin, USA. *Sci Total Environ* 568:404–414
- CRM (1996) Informe final complementario a la cartografía geológico-minera y geoquímica escala 1:50,000. Hoja Santa María del Oro (F13-D32) Estado de Nayarit. Consejo de Recursos Minerales, p 24. [https://www.sgm.gob.mx/publicaciones\\_sgm/Informe\\_b.jsp?wparam=1&clav=181996CECR0001](https://www.sgm.gob.mx/publicaciones_sgm/Informe_b.jsp?wparam=1&clav=181996CECR0001)
- Davison W (1993) Iron and manganese in lakes. *Earth Sci Rev* 34:119–163
- Díaz-Asencio M, Sanchez-Cabeza JA, Ruiz-Fernández AC, Corcho-Alvarado JA, Pérez-Bernal LH (2020) Calibration and use of well-type germanium detectors for low-level gamma-ray spectrometry of sediments using a semi-empirical method. *J Environ Radioact* 225:1–10
- Dokulil MT (2013) Environmental impacts of tourism on lakes. In: Ansari A, Gill S (eds) *Eutrophication: causes, consequences and control*. Springer, Dordrecht, pp 81–88
- Filzmoser P, Hron K, Templ M (2018) *Applied compositional data analysis*. With worked examples in R. Springer, Switzerland
- García E (1973) *Modificaciones al sistema de clasificación climática de Köppen (para adaptarlo a las condiciones de la República Mexicana)*. Universidad Nacional Autónoma de México, México

- Gierlowski-Kordesch EH (2010) Lacustrine carbonates. In: Alonso-Zarza AM, Tanner LH (eds) *Developments in sedimentology*, vol 61. Elsevier, Amsterdam, pp 1–101
- Gómez-Cancino CK (2016) La minería en Nayarit, un recorrido histórico. *Cienciamx Noticias*, Agencia Informativa CONACYT. <http://www.cienciamx.com/index.php/tecnologia/tic/10986-la-mineria-en-nayarit-un-recorrido-historico>
- González-Bernal VM (2008) Problemática socioeconómica de los productores independientes de agave azul del municipio de Santa María del Oro, Nayarit, 1996–2006. Dissertation. Universidad Autónoma de Nayarit. Tepic, p 115
- Gorny J, Billon G, Noiriél C, Dumoulin D, Lesven L, Madé B (2016) Chromium behavior in aquatic environments: a review. *Environ Rev* 24:503–516
- Hair JF Jr, Black WC, Babin BJ, Anderson RE (2014) *Multivariate data analysis*, 7th edn. Pearson Education Limited, Essex
- Hernández Cerda ME, Valdez Madero G (2004) Sequía meteorológica. In: Martínez J, Fernández Bremauntz A (eds) *Cambio climático: una visión desde México*. Instituto Nacional de Ecología, Mexico City
- Hernández-Rivera DM (2018) Niveles de contaminación por metales pesados en sedimentos de los lagos El Sol y La Luna, en el volcán Nevado de Toluca, México. Instituto Tecnológico de Mazatlán. México, p 87
- Horowitz AJ (1985) *A primer on trace metal-sediment chemistry*. Water Supply Paper 2277. United States Geological Survey, Alexandria
- Howard HH, Chisholm SW (1975) Seasonal variation of manganese in a eutrophic lake. *Am Midl Nat* 93:188–197
- INAFED (2010) Santa María del Oro. *Enciclopedia de los Municipios y Delegaciones de México*. Instituto Nacional para el Federalismo y el Desarrollo Municipal. <http://www.inafed.gob.mx/work/enciclopedia/EMM18nayarit/municipios/18014a.html>
- INEGI (2017) *Anuario estadístico y geográfico de Nayarit 2017*. Instituto Nacional de Estadística y Geografía, Aguascalientes
- INIFAP (2012) Programa de acción ante el cambio climático de Nayarit. Resumen ejecutivo. Instituto Nacional de Investigaciones Forestales, Agrícolas y Pecuarias. Tepic
- Jeppesen E, Meerhoff M, Davidson TA, Trolle D, Soendergaard M, Lauridsen TL, Beklioglu M, Brucet S, Volta P, Gonzalez-Bergonzoni I, Nielsen A (2014) Climate change impacts on lakes: an integrated ecological perspective based on a multi-faceted approach, with special focus on shallow lakes. *J Limnol* 73:84–107
- Johnson JE, Webb SM, Ma C, Fischer WW (2016) Manganese mineralogy and diagenesis in the sedimentary rock record. *Geochim Cosmochim Acta* 173:210–231
- Kamennaya NA, Ajo-Franklin CM, Northen T, Jansson C (2012) Cyanobacteria as biocatalysts for carbonate mineralization. *Minerals* 2:338–364
- Krishnaswamy S, Lal D, Martin JM, Meybeck M (1971) Geochronology of lake sediments. *Earth Planet Sci Lett* 11:407–414
- Laquatra J (2014) Lead in household products. In: Snedeker S (ed) *Toxicants in food packaging and household plastics*. Molecular and Integrative Toxicology. Springer, London, pp 231–243
- Lefkowitz JN, Varekamp JC, Reynolds RW, Thomas E (2017) A tale of two lakes: the Newberry Volcano twin crater lakes, Oregon, USA. In: Ohba T, Capaccioni B, Caudron C (eds) *Geochemistry and geophysics of active volcanic lakes*. *Geol Soc Spec Publ* 437: 253–288
- Li K, Liu E, Zhang E, Li Y, Shen J, Liu X (2017) Historical variations of atmospheric trace metal pollution in Southwest China: Reconstruction from a 150-year lacustrine sediment record in the Erhai Lake. *J Geochem Explor* 72:62–70
- Li X, Liu E, Zhang E, Lin Q, Yu Z, Nath B, Yuan H, Shen J (2020) Spatio-temporal variations of sedimentary metals in a large suburban lake in southwest China and the implications for anthropogenic processes. *Sci Total Environ* 707:1–46
- Lin Q, Liu E, Zhang E, Nath B, Shen J, Yuan H, Wang R (2018) Reconstruction of atmospheric trace metals pollution in Southwest China using sediments from a large and deep alpine lake: Historical trends, sources and sediment focusing. *Sci Total Environ* 613–614:331–341
- Lintern A, Leahy P, Heijnis H, Zawadzki A, Gadd P, Jacobsen G, Deletic A, Mccarthy D (2016) Identifying heavy metal levels in historical flood water deposits using sediment cores. *Water Res* 105:34–46
- Loring D, Rantala R (1992) *Manual for the geochemical analyses of marine sediments and suspended particulate matter*. *Earth Sci* 32:235–283
- MacDonald DD, Carr RS, Calder FD, Long ER, Ingersoll CG (1996) Development and evaluation of sediment quality guidelines for Florida coastal waters. *Ecotoxicology* 5:253–278
- Magalhães MCF (2002) Arsenic. An environmental problem limited by Solubility. *Pure Appl Chem* 74:1843–1850
- Malkiewicz M, Waroszewski J, Bojko O, Egli M, Kabala C (2016) Holocene vegetation history and soil development reflected in the lake sediments of the Karkonosze Mountains (Poland). *SAGE Open Med* 26:890–905
- Manav R, Görgün A, Isik F (2016) Radionuclides ( $^{210}\text{Po}$  and  $^{210}\text{Pb}$ ) and some heavy metals in fish and sediments in lake Bafa, Turkey, and the contribution of  $^{210}\text{Po}$  to the radiation dose. *Int J Environ Res Public Health* 13:1–11
- Matschullat J, Ottenstein R, Reimann C (2000) Geochemical background - can we calculate it? *Environ Geol* 39:990–1000
- Meena N, Prakasam M, Bhushan R, Sarkar S, Diwate P, Banerji U (2017) Last-five-decade heavy metal pollution records from the Rewalsar Lake, Himachal Pradesh, India. *Environ Earth Sci* 76:1–10
- Mna H, Oueslati W, Helali M, Zaaboub N, Added A, Aleya L (2017) Distribution and assessment of heavy metal toxicity in sediment cores from Bizerte Lagoon. *Tunisia Environ Monit Assess* 189:1–18
- Moreno-Moreno LR, Orozco-Espinosa P, Barrón Arreola KS (2015) Turismo y medio ambiente. Una aplicación del método de costo de viaje en la Laguna de Santa María del Oro, Nayarit. In: Barrón-Arreola KS, Fonseca-Morales

- MA (eds) *Temas selectos de turismo y sustentabilidad*. Universidad Autónoma de Nayarit, Tepic
- Murray JW, Berry Spell B, Paul B (1983) The contrasting geochemistry of manganese and chromium in the Eastern tropical Pacific Ocean. In: Wong CS et al (eds) *Trace metals in sea water*. Springer, New York, pp 643–669
- Neff JM (2002) *Bioaccumulation in marine organisms. Effect of contaminants from oil well produced water*. Elsevier, The Netherlands
- Nicomel NR, Leus K, Folens K, Van Der Voort P, Du Laing G (2015) Technologies for arsenic removal from water: current status and future perspectives. *Int J Environ Res Public Health* 13(62):2–24
- Nooripoor M, Khosrowjerdi M, Rastegari H, Sharifi Z, Bijani M (2021) The role of tourism in rural development: evidence from Iran. *GeoJournal* 86:1705–1719
- Ongley ED (1996) *Control of water pollution from agriculture. FAO irrigation and drainage paper 55. Food and Agriculture Organization of the United Nations, Rome*, p 101. <http://www.fao.org/3/w2598e/w2598e00.htm#Contents>
- Ontiveros-Cuadras J, Ruiz-Fernández A, Sanchez-Cabeza J, Pérez-Bernal L, Sericano J, Preda M, Liong Wee Kwong L, Páez-Osuna F (2014) Trace element fluxes and natural potential risks from 210Pb-dated sediment cores in lacustrine environments at the Central Mexican Plateau. *Sci Total Environ* 469:677–687
- Panagiotaras D, Nikolopoulos D (2015) Arsenic occurrence and fate in the environment; a geochemical perspective. *J Earth Sci Clim Change* 6:1–9
- Pedersen TF, Vogel JS, Southon JR (1986) Copper and manganese in hemipelagic sediments at 21°N, East pacific rise: diagenetic contrasts. *Geochim Cosmochim Acta* 50:2019–2031
- Pelletier N, Chételat J, Blarquez O, Vermaire JC (2020) Paleolimnological assessment of wildfire-derived atmospheric deposition of trace metal(loid)s and Major Ions to Subarctic Lakes (Northwest Territories, Canada). *J Geophys Res Biogeosci* 125(8):e2020JG005720
- PO (2003) Acuerdo por el que se expide el programa de ordenamiento ecológico de la cuenca de Santa María del Oro, Nayarit. *Periodico Oficial* (12 febrero 2003), CLXXII—19, Tepic
- Reczyński W, Szarłowicz K, Jakubowska M, Bitusik P, Kubica B (2020) Comparison of the sediment composition in relation to basic chemical, physical, and geological factors. *Int J Sediment Res* 35:307–314
- Renard F, Putnis CV, Montes-Hernandez G, Ruiz-Agudo E, Hovelmann J, Sarret G (2015) Interactions of arsenic with calcite surfaces revealed by in situ nanoscale imaging. *Geochim Cosmochim Acta* 159:61–79
- Rinklebe J, Shaheen SM (2017) Redox chemistry of nickel in soils and sediments: a review. *Chemosphere* 179:265–278
- Robbins JA (1978) Geochemical and geophysical applications of radioactive lead. In: Nriagu JO (ed) *Biogeochemistry of lead in the environment*. Elsevier Scientific, Amsterdam
- Rodríguez-Ramírez A, Caballero M, Roy P, Ortega B, Vázquez-Castro G, Lozano-García S (2015) Climatic variability and human impact during the last 2000 years in western Mesoamerica: evidences of late Classic and Little Ice Age drought events. *Clim past* 11:1239–1248
- Rose NL, Yang H, Turner SD, Simpson GL (2012) An assessment of the mechanisms for the transfer of lead and mercury from atmospherically contaminated organic soils to lake sediments with particular reference to Scotland, UK. *Geochim Cosmochim Acta* 82:113–135
- Ruiz-Fernández AC, Páez-Osuna F, Urrutia-Fucugauchi J, Preda M, Rehault I (2004) Historical trace metal fluxes in the Mexico City Metropolitan Zone as evidenced by a sedimentary record from the Espejo de los Lirios lake. *J Environ Monit* 6:473–480
- Ruiz-Fernández AC, Hillaire-Marcel C, Páez-Osuna F, Ghaleb B, Caballero M (2007) <sup>210</sup>Pb chronology and trace metal geochemistry at Los Tuxtlas, Mexico, as evidenced by a sedimentary record from the Lago Verde Crater Lake. *Quat Res* 67:181–192
- Ruiz-Fernández AC, Hillaire-Marcel C (2009) <sup>210</sup>Pb-derived ages for the reconstruction of terrestrial contaminant history into the Mexican Pacific coast: potential and limitations. *Mar Pollut Bull* 59:134–145
- Ruiz-Fernández AC, Maanan M, Sanchez-Cabeza JA, Pérez-Bernal LH, López-Mendoza P, Limoges A (2014) Cronología de la sedimentación reciente y caracterización geoquímica de los sedimentos de la laguna de Alvarado, Veracruz (suroeste del golfo de México). *Cienc Mar* 40:291–303
- Ruiz-Fernández AC, Sanchez-Cabeza JA, Blaauw M, Pérez-Bernal LH, Cardoso-Mohedano JG, Aquino-López MA, Keaveney E, Giral S (2022) Historical reconstruction of sediment accumulation rates as an indicator of global change impacts in a tropical crater lake. *J Paleolimnol*
- Sageman BB, Lyons TW (2004) Geochemistry of fine-grained sediments and sedimentary rocks. In: MacKenzie F (ed) *Sediments, diagenesis, and sedimentary rocks. Treatise on geochemistry, vol 7*. Elsevier, New York, pp 115–158
- Sahoo GB, Schladow SG (2008) Impacts of climate change on lakes and reservoirs dynamics and restoration policies. *Sustain Sci* 3:189–199
- Salomons W, Förstner U (1984) *Metals in the hydrocycle*. Springer, Berlin
- Sanchez-Cabeza JA, Ruiz-Fernández AC (2012) <sup>210</sup>Pb sediment radiochronology: an integrated formulation and classification of dating models. *Geochim Cosmochim Acta* 82:183–200
- Sanchez-Cabeza JA, Ruiz-Fernández AC, Ontiveros-Cuadras JF, Pérez-Bernal LH, Olid C (2014) Monte Carlo uncertainty calculation of <sup>210</sup>Pb chronologies and accumulation rates of sediments and peat bogs. *Quat Geochronol* 23:80–93
- Schaufelberger FA (1994) Arsenic minerals formed at low temperatures. In: Nriagu JO (ed) *Arsenic in the environment*. Wiley, New York, pp 403–415
- SEDATU (2013) *Atlas de riesgos del municipio de Santa María del Oro, Nayarit*. Secretaría de Desarrollo Agrario, Territorial y Urbano NAY-SAMAO-PRAH-04-0012013. Tepic
- Serrano D, Filonov A, Tereshchenko I (2002) Dynamic response to valley breeze circulation in Santa María

- del Oro, a volcanic lake in Mexico. *Geophys Res Lett* 29:27–31
- SGM (2020) Panorama Minero del Estado de Nayarit. Secretaría de Minería. Servicio Geológico Mexicano. <http://www.sgm.gob.mx/pdfs/NAYARIT.pdf>
- Smedley PL, Kinniburgh DG (2002) A review of the source, behaviour and distribution of arsenic in natural waters. *Appl Geochem* 17:517–568
- SMN (2020) Normales Climatológicas por Estado/Nayarit. Servicio Meteorológico Nacional, Comisión Nacional del Agua. <https://smn.conagua.gob.mx/es/informacion-climatologica-por-estado?estado=nay>. Accessed 28 May 2020
- Smol JP (2008) Pollution of lakes and rivers. A paleoenvironmental perspective. Blackwell Publishing, Malden
- Stahn C, Iverson J, Easterday JS (2017) Environmental protection and transitions from conflict to peace: clarifying norms, principles, and practices. Oxford University Press, Oxford
- Steffen W, Sanderson A, Tyson PD, Jäger J, Matson PA, Moore BIII, Oldfield F, Richardson K, Schellnhuber HJ, Turner IIBL, Wasson RJ (2005) Global change and the earth system. A planet under pressure. Springer, New York
- Tapia J, Audry S (2013) Control of early diagenesis processes on trace metal (Cu, Zn, Cd, Pb and U) and metalloid (As, Sb) behaviors in mining-and smelting-impacted lacustrine environments of the Bolivian Altiplano. *Appl Geochem* 31:60–78
- Templ M, Hron K, Filzmoser P, Facevicova K, Kynclova P, Walach J, Pintar V, Chen J, Miksova D, Meindl B, Menafoglio A, Di Blasi A, Pavone F, Stefelova N, Zeni G (2021) Package robCompositions: compositional data analysis (version 2.3.1.). <https://cran.r-project.org/web/packages/robCompositions/>
- UrbanErnst NRK, Bernasconi S (1999) Addition of sulfur to organic matter during early diagenesis of lake sediments. *Geochim Cosmochim Acta* 63:837–853
- USGS (2020) Water science school: lakes and reservoirs. United States Geological Service. [https://www.usgs.gov/special-topic/water-science-school/science/lakes-and-reservoirs?qt-science\\_center\\_objects=0#qt-science\\_center\\_objects](https://www.usgs.gov/special-topic/water-science-school/science/lakes-and-reservoirs?qt-science_center_objects=0#qt-science_center_objects)
- Valencia-Plascencia MA, Jacome-Pérez BG (1993) Cultivo experimental de tilapia (*Oerochromis aureus*) en jaulas flotantes de P.V.C. en el lago de Santa María del Oro, Nay. Bachelor's dissertation. Universidad Autónoma de Nayarit, Tepic, p 47
- Van der Weijden CH (2002) Pitfalls of normalization of marine geochemical data using a common divisor. *Mar Geol* 184(3–4):167–187
- Veizer J (1983) Trace elements and isotopes in sedimentary carbonates. *Rev Mineral Geochem* 11:265–299
- Yang H, Rose N (2005) Trace element pollution records in some UK lake sediments, their history, influence factors and regional differences. *Environ Int* 31:63–75
- Zhang H, Huo S, Yeager KM, Xi B, Zhang J, He Z, Ma C, Wu F (2018) Accumulation of arsenic, mercury and heavy metals in lacustrine sediment in relation to eutrophication: Impacts of sources and climate change. *Ecol Indic* 93:771–780
- Zhu YG, Xue XM, Kappler A, Rosen BP, Meharg AA (2017) Linking genes to microbial biogeochemical cycling: lessons from arsenic. *Environ Sci Technol* 51:7326–7339

**Publisher's Note** Springer Nature remains neutral with regard to jurisdictional claims in published maps and institutional affiliations.

Springer Nature or its licensor holds exclusive rights to this article under a publishing agreement with the author(s) or other rightsholder(s); author self-archiving of the accepted manuscript version of this article is solely governed by the terms of such publishing agreement and applicable law.